

HEFAT2010
7th International Conference on Heat Transfer, Fluid Mechanics and Thermodynamics
19-21 July 2010
Antalya, Turkey

EXPERIMENTAL INVESTIGATION OF TURBULENT BOUNDARY LAYER SEPARATION IN ADVERSE PRESSURE GRADIENT

Behfarshad G.* and Jafarian A.S

*Author for correspondence

Department of Mechanical and Aerospace Engineering,
Science and Research Branch, Azad University,
Tehran, 1477893855,
Iran,

E-mail: behfarshad@srbiau.ac.ir

ABSTRACT

The problem of turbulent boundary-layer separation due to an adverse pressure gradient is an important factor in the design of many devices such as jet engines, rocket nozzles, airfoils and helicopter blades and the design of many fluidic logic systems. As a result, wind tunnel experiments were conducted to investigate the separation developing on a flat-plate in steady and unsteady flow. The nature of upstream flow subjected to the effect of unsteady freestream velocity which changes sinusoidally with time due to the rotation of an elliptical cylinder placed downstream of the flat plate has been studied in the test section. Separation points (or line) were measured in different angles of incidence and at various stations. Pitot-static tube and hot-wire anemometry were used to measure the steady and instantaneous velocities and turbulence. The results indicate that the more the increase in the angle of incidence of the flat plate in steady and unsteady flow, the more is the increase in the thickness of separated region which extends further towards the flat plate trailing edge. Reduced frequency also causes the separation points to move up away from the surface of the flat plate but this movement is restricted to reduced frequencies less than 2 after which the changes are negligible.

INTRODUCTION

One of the most difficult problems encountered in the calculation of practical unsteady flows is that of predicting boundary layer separation [1].

Separation in fluid mechanical term is generally used to describe the detachment of a flow from a surface. Flow separation occurs when the boundary layer travels far enough and against wall friction and an adverse pressure gradient that the speed of the boundary layer falls almost to zero. The fluid flow becomes detached from the surface of the object, and instead takes the forms of eddies and vortices. In aerodynamics, flow separation can often result in increased drag, particularly

pressure drag which is caused by the pressure differential between the front and rear surfaces of the object as it travels through the fluid [2]. For this reason much effort and research has gone into the design of aerodynamic and hydrodynamic surfaces which delay flow separation and keep the local flow attached for as long as possible.

At separation, the rotational flow region next to the wall abruptly thickens, the normal velocity component increases, and the boundary-layers approximations are no longer valid.

Separation can be triggered experimentally with concentrated vortices moving close to a wall. Harvey and Perry placed a half-span rectangular wing in a wind tunnel and observed the evolution of the resulting single trailing vortex as it passes over a downstream moving floor. Total-head surveys in planes across the flow were conducted to observe separation and the formation of a secondary vortex of opposite sense to the main one. The secondary vortex causes a rebounding of the trailing vortex [3]. Similar effects are present when a ring vortex approaches a wall normal to its propagation direction [4,5]. In the latter case a downstream-moving unsteady separation is produced.

Simpson [6] conducted experiments on steady and unsteady separation in turbulent flows. They investigated the structure of separating, nominally two-dimensional, turbulent boundary layers in a steady freestream as well as in a sinusoidally oscillating freestream. Upstream of where intermittent backflow begins, the flow behaves in a quasi steady manner. Downstream, there are non-quasi steady effects on the ensemble-averaged velocity profiles which are more pronounced for higher-reduced-frequency freestream oscillations.

Didden and Ho[7] conducted measurement of the downstream-moving separation caused by periodic ring vortices impinging normally onto a flat plate.

Ho[8] attributes the sparseness of a positive experimental proof of the criterion for unsteady separation to the difficulty of

2 Topics

measuring the separated velocity near the wall. The temporal variation of the resulting three-dimensional velocity field necessitates the use of a large number of small, fast-response probes and a colossal data acquisition and storage system. This problem is particularly acute for an upstream moving separation, where flow reversal occurs leading to additional measuring difficulties. No flow reversal occurs in a downstream moving separation, and hot-wire probes can then be used to survey the flow field in the vicinity of the wall.

Great strides have been made in the past few decades in establishing a firm analytical foundation for steady, two dimensional separations. On the other hand, three dimensional or unsteady separation represents a domain of fluid mechanics that is presently beyond the reach of definitive theoretical or numerical analysis, and progress to date has depended crucially on experimental work [9].

An implicit formula for boundary current separation was derived for downstream variation in velocity and pressure of an ocean boundary current by Marshal and Tansley [10]. Boundary layer separation in adverse pressure gradient in engine inlet and ducts has also been studied experimentally by Kumar and Alvi [11]. They found that activating arrays of 400 μm microjets can attach the flow significantly.

In order to perform the experiments in unsteady turbulent boundary layer, a reliable data acquisition system is required. The present project was therefore started by installing and commissioning a new data acquisition system. Once the data acquisition system was in working order, hot-wire measurement on unsteady case were carried out. These results were then used to study the nature of steady and unsteady flow in the wind tunnel.

NOMENCLATURE

| | | |
|--------|----------------------|---|
| c | [m] | Airfoil chord |
| p | [N/m ²] | pressure |
| Re | [] | Reynolds number |
| U | [m/s] | instantaneous velocity component in the x direction |
| x | [m] | longitudinal distance from leading edge |
| y | [m] | vertical distance from the wing surface |
| H | [m] | wind tunnel test section height |
| ρ | [kg/m ³] | Air density |
| k | [$\omega c/2U$] | Reduced Frequency |

| | | |
|--------------------|-------|-------------------------------|
| Special characters | | |
| α | [deg] | flat-plate angle of incidence |

| | | |
|------------|--|---------|
| Subscripts | | |
| d | | Dynamic |

EXPERIMENTAL SETUP

A subsonic open circuit wind tunnel was used to investigate the unsteady turbulent boundary layer separation developing on a flat-plate at different angles of incidence.

The dimensions of the test section were 460 mm x 460 mm x 1220 mm and the flat-plate with the chord length of 200 mm and thickness of 4 mm was installed at the mid position of this section. Provision was made to rotate the flat-plate about 1/4 of the leading edge to give a mean geometric angle of incidence of between zero to 25 degree. Just downstream of the trailing edge a two dimensional elliptical cylinder ($L=455$ mm, $b/a=2$, where L

is the length, ' $b=50\text{mm}$ ' is the major diameter and ' a ' is the minor diameters) was located with its axis at $x/c=0.175$, $y/c=0.2$ where in this case $x=y=0$ at the wing trailing edge.

In order to create different reduced frequency, the elliptical cylinder was rotated from zero to 1800 r.p.m. through a belt driven by an adjustable speed electric motor and on the other side of the shaft elliptical cylinder was coupled to a photocell sensor which produces a pulse train viewing the elliptical cylinder shaft. This provides the control on cylinder rotational speed and an unsteady perturbation to the flow around the flat-plate. Roughness was applied to the cylinder in order to delay separation on its surface. The elliptical cylinder shaft and all accessories were installed on a main frame.

Velocity measurements were carried out by pitot-static-tube and hot wire anemometer mounted on a traversing gear. Total and static pressures of pitot static tube (1.7 mm in diameter) were fed into a transducer connected to a digital manometer. Hot-wire velocities were measured by a 5 (μm) platinum-plated tungsten constant-temperature DANTEC 55P15 hot-wire anemometer using a single hot wire (determining longitudinal velocity). In any case the hot wire probe was traversing the flat-plate. Because of mechanical limitations, pitot static tube could not go further up from $x/c=0.3$ to the leading edge, thus measurement was carried out at four stations towards trailing edge of the flat plate, but it was possible with hot-wire probe to do the measurement at $x/c=0.1$. The traversing gear used for this probe was designed specifically for this experiment.

For the experiments it was necessary to acquire the signals coming from hot wire and store them in the computer memory. Also two data acquisition boards, HSDAS-12 (products from Analogic Corporation) and PC-812PG (products from Advantech Co.,Ltd.) were installed in computers. Two data acquisition softwares named LABTECH NOTEBOOK, Ver.7.1.0,(a product from Laboratory Technologies Corporation) and SNAPSHOT Storage Scope, (from Snap-series Software by HEM Corporation) were bought and used for data acquisition. Figure 1 shows a view of the experimental set up.

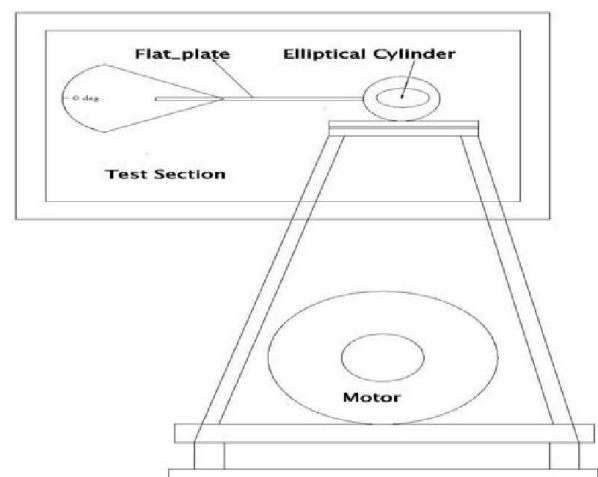


Figure 1 Experimental setup

MEASUREMENT TECHNIQUES

Mean velocity profiles were measured for steady flow by pitot-static-tube and hot-wire in three different stages.

At first stage the effect of cylinder on the upstream velocity was studied. In this stage the flat-plate was removed from the wind tunnel and the elliptic cylinder was fixed horizontally on its major axis. The velocity distributions were measured by a tiny pitot-static-tube in the wind tunnel from up to bottom of test section for three velocities 15m/s, 20m/s and 30m/s at different positions relative to the leading edge position of the flat-plate($x/c=0.3, x/c=0.5, x/c=0.7, x/c=0.9$). The dynamic pressure from the pitot-static-tube was then converted to velocity.

In the second stage, the elliptic cylinder was then removed from the test section. Then velocity distribution was investigated by pitot-static tube for different angles of incidence (4, 5, 6, 7, 10 degs.) and at various positions (above the wing) from the flat plate leading edge ($x/c=0.3, x/c=0.5, x/c=0.7, x/c=0.9$). This experiment was performed for two free stream velocities (20m/s, 30m/s).

In the third stage the effect of stationary cylinder on the flat-plate was studied. Flat plate was positioned at different angles of incidence (5, 6, 7, 10 degs.) and the velocity distributions were measured over and under of it. These experiments were done at those stations mentioned above in velocities 20m/s and 30m/s. For measuring the velocity profile under the flat plate, the flat plate was positioned in negative angle of incidence and measurement was carried out on its surface. Then correction for height was taken into account.

Figure 2 shows a diagram of the data acquisition system used in relation to the hot-wire measurement.

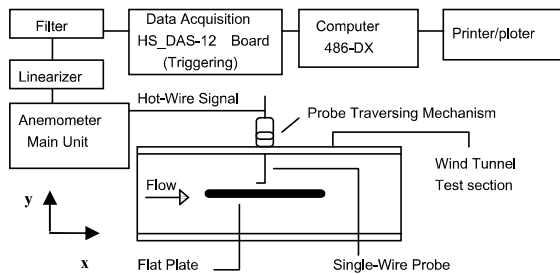


Figure 2 Data acquisition system

EXPERIMENTAL RESULT

Velocity Measurements by Pitot Static Tube

Figure 3 shows the velocity distribution in the wind tunnel test section for different stations in the absence of flat plate. As can be seen in these graphs, because the elliptic cylinder is present in the test section the upstream flow is retarded at the plane of cylinder. The effect is greater when getting closer to the ellipse.

Figure 4 illustrates the velocity distribution above the wing when it is subjected to $\alpha=4\text{deg}$ in the absence of elliptical cylinder. As can be seen from this figure, the flow is attached to the surface and the velocity profile for $x/c=0.7$ is found to be similar to that of a turbulent boundary layer.

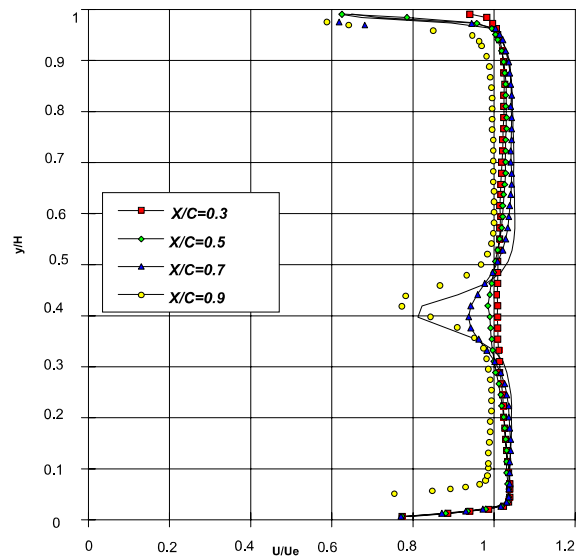


Figure 3 Velocity distribution in the wind tunnel test section in the absence of flat plate at different station, $U_e=30\text{m/s}, k=0$

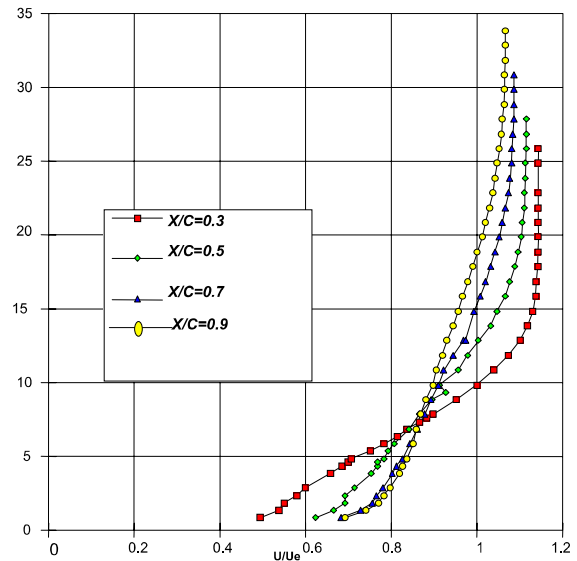


Figure 4 Velocity distribution in the absence of cylinder for $U_e=30\text{m/s}, \alpha=4\text{deg}$

Figure 5 shows a specific velocity distribution for different angles of incidence in the absence of cylinder. The point of separation, zero velocity, is shown in these figures. As the angle of incidence starts increasing, the separation region gets thicker and extended more towards the trailing edge. In fact fluid particles in the boundary layers have slowed down by wall friction and adverse pressure gradient due to increase in angle of incidence. As the external potential flow is sufficiently retarded by the presence of an adverse pressure gradient, the

2 Topics

momentum of those particles is consumed by both the wall shear and the pressure gradient. So at some point the viscous layer departs from the boundary surface and as a result, separation of flow occurs. The increase in angle of incidence would cause the adverse pressure gradient to grow faster and consequently, the separation area develops furthermore and would move towards the wing leading edge. In this case study (Figure 5), the separation region is nearly finished at about $x/c=0.9$.

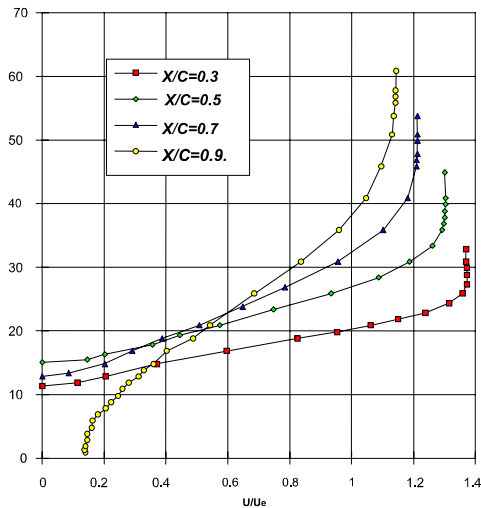


Figure 5 Velocity distribution in the absence of cylinder for $U_e=30\text{m/s}$, $\alpha=7\text{deg}$

The effect of different free stream velocity is shown in Figure 6 and it shows that higher upstream velocity will cause to increase the separation height from the surface of the flat plate. As can be seen increasing velocity by 10m/s has caused about 2mm growth in separation area thickness.

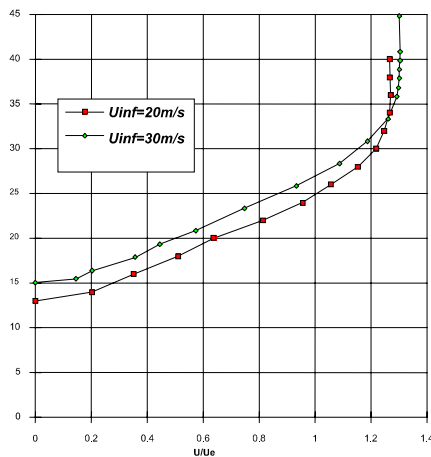


Figure 6 Velocity distribution for different velocities in the absence of cylinder, $\alpha=7\text{deg}$, $x/c=0.5$

Separation line for different angles of incidence (when the cylinder is present but not rotating) is shown in Figure 7. As was expected, higher incidence angle causes thicker separated region which extends further downstream on the flat plate. Unfortunately, beyond $x/c=0.3$ and $x/c=0.95$, no measurement could be performed due experimental setup limitations. As it can be seen from this figure, the mid-wing station ($x/c=0.5$), is in the separation area for angles of incidence greater than 5 degrees.

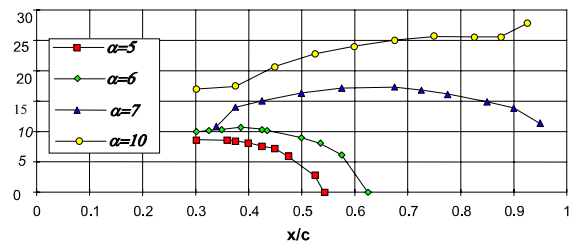


Figure 7 Approximate line of separation for different angles of incidence for $U_e=30\text{m/s}$, $k=0$

In Figure 8 the effect of changing reduced frequency which comes from the rotation of elliptical cylinder, at the station of mid-wing position -in the absence of the wing- has been illustrated. As can be seen from this figure, there is negligible change due to increase in the reduced frequency. Also it can be seen from Figure 9, there is no great change due to the increase in the free stream velocity at the moderate reduced frequency ($k=2$).

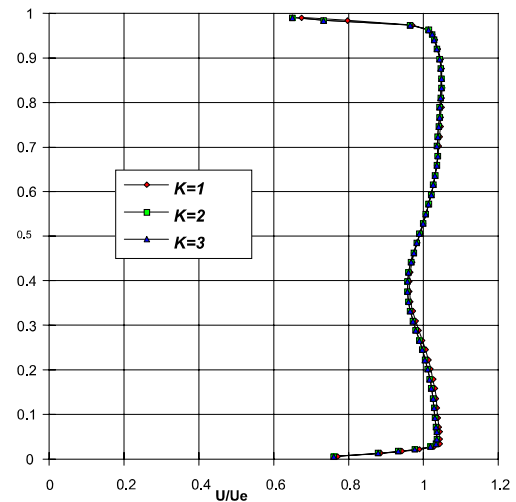


Figure 8 Velocity distribution in the wind tunnel section at different reduced frequencies, $U_e=30\text{m/s}$, $x/c=0.5$

As a typical velocity profile for $\alpha=6\text{deg}$ and $U=30\text{m/s}$, velocity distribution in different position above the wing subjected to the medium reduced frequency ($k=2$) has been shown in Figure 10. As it is shown in this figure, the height of the separation zone is more at the mid-wing($x/c=0.5$) and it reduces as the region spreads further towards the trailing edge.

Also the effect of reduced frequency causes the separation points to move up about 4mm and this is clearly observed when compared with the same situation without the presence of elliptical cylinder in the wind tunnel test section. This feature is shown in Figure 11.

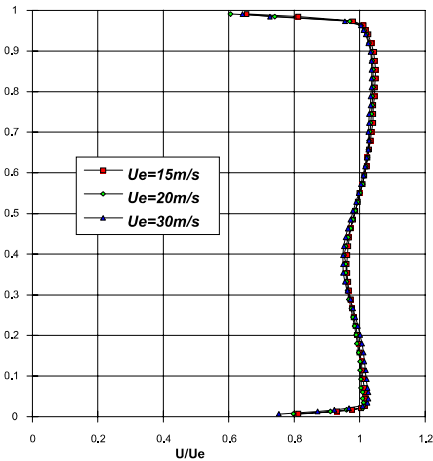


Figure 9 Velocity distribution in the wind tunnel section at different free stream velocities, $x/c=0.3$, $k=2$

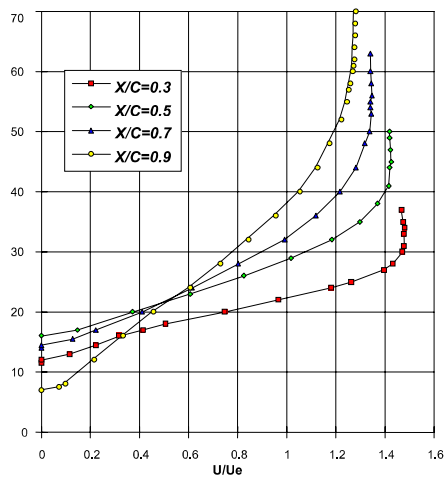


Figure 10 Velocity distribution for $U_e=30\text{m/s}$, $\alpha=6\text{deg}$, $k=2$

Figure 12 shows the separation points in different angle of incidence. The separation point moves up and the boundary layer thickness increases as the angle of incidence increases. This is due to the development and thickening of the separation region occurring above the wing.

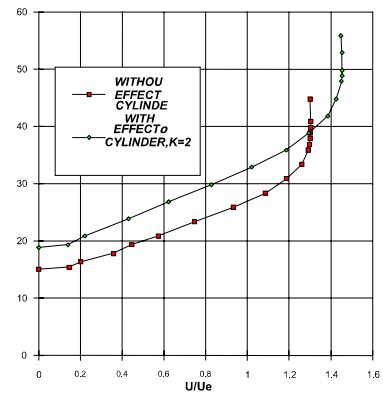


Figure 11 Velocity distribution with and without the effect of cylinder for $U_e=30\text{m/s}$, $\alpha=7\text{deg}$, $x/c=0.5$

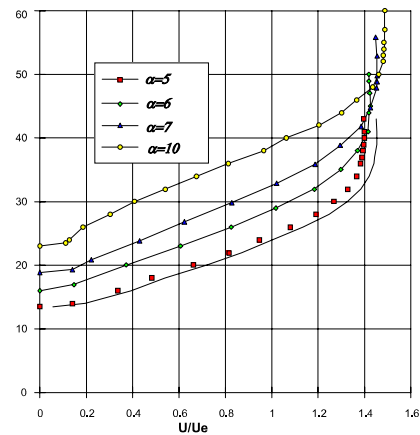


Figure 12 velocity distribution in different angles of incidence for $U_e=30\text{m/s}$, $x/c=0.5$, $k=2$

Figure 13 shows the effect of various reduced frequencies. The effect of reduced frequency in increasing the separation height is not that much and it seems to stop at some stage. As can be seen, further increases in reduced frequency do not change the separation height anymore.

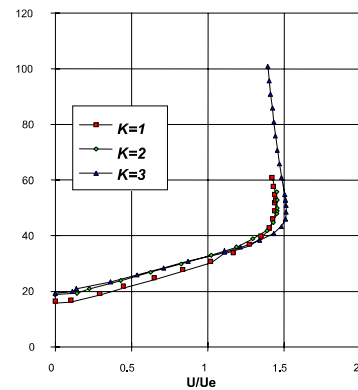


Figure 13 Velocity distribution in different reduced frequencies for $U_e=30\text{m/s}$, $\alpha=7\text{deg}$, $x/c=0.5$

Mean and Unsteady Velocity Measurements by Hot-Wire Anemometry

Measurements of the velocities induced by elliptical cylinder in the plane of the flat plate chord (without the flat plate in the wind tunnel) show that a sinusoidal velocity variation is produced by the facility and the perturbation is dominated by an unsteady up wash concentrated mostly near the flat plate trailing edge(see Figure 14).

This unsteady velocity measurements recorded by data acquisition system is presented in Figure 14 for a particular condition ($U=30$ m/s, $x/c=0.7$ and $k=2$) as an example.

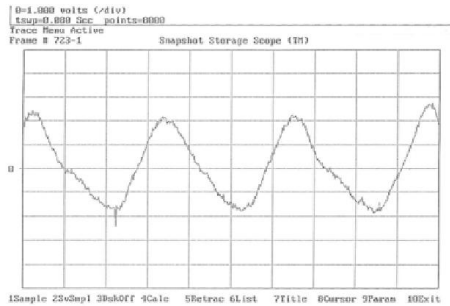


Figure 14 Velocity flow perturbation in the plane of the flat plate for $U_e=30$ m/s, $x/c=0.7$, $k=2$

In order to check the results, pitot-static-tube measurements were also compared with the mean hot-wire results which found to agree within 93 percent. This suggested a good reliability of the measurements.

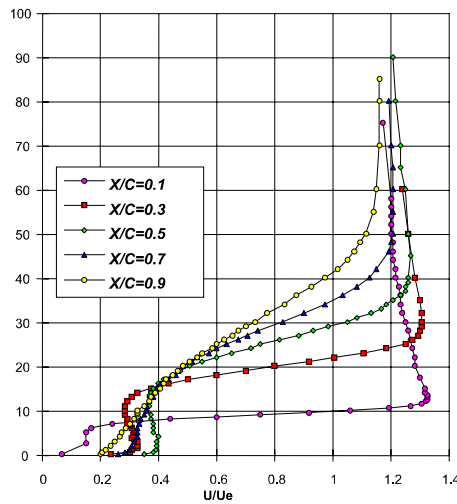


Figure 15 Velocity distribution with hot-wire for $U_e=30$ m/s, $\alpha=7$ deg, $k=2$

Figure 15 shows the mean velocity measurements obtained by hot-wire anemometry for different stations on top of the wing starting from $x/c=0.1$ to $x/c=0.9$. These results were obtained simply by reading the analogue readouts on the hot-wire anemometer. As can be seen the approximate height of

separation region is about 17mm from the wing surface and the separation zone seems to finished at $x/c=0.9$.

Figure 16 shows the ensemble averaged velocity profile for different angle of incidence over the flat plate at the mid-wing position. As it is expected, the higher the angle of incidence, the thicker was the separation region. Time averaged velocity profile for different angles of incidence was also calculated and it is exactly looked like the ensemble averaged.

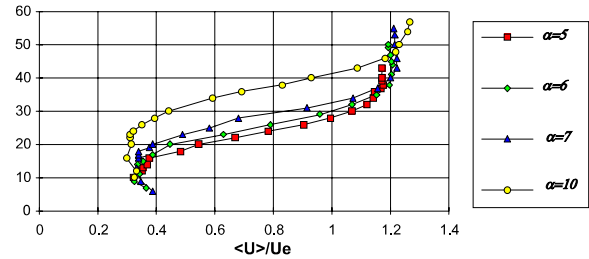


Figure 16 Ensemble averaged velocity profile for different angles of incidence, $U_e=30$ m/s, $x/c=0.5$, $k=2$

Figure 17 shows the effect of reduced frequency. Again as is expected the effect of reduced frequency at $k=3$ is not much more than that of $k=2$ which is in compromise with the finding of figure 13.

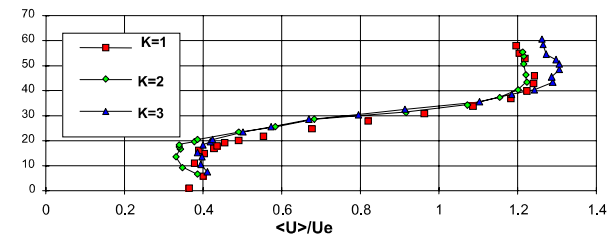


Figure 17 Ensemble averaged velocity profile for different reduced frequencies, $U_e=30$ m/s, $\alpha=7$ deg, $x/c=0.5$

Figure 18 shows the effect of increasing free stream velocity. It can be observed that at a fixed reduced frequency, the thickening of separation region is more in the low velocities. It is due to the lesser energy or momentum of the incoming flow to overcome the effect of adverse pressure gradient and wall skin friction.

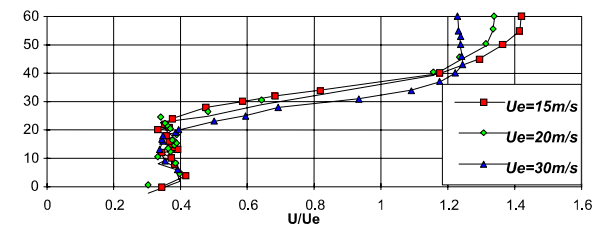


Figure 18 Ensemble averaged velocity profile for different free stream velocity for $\alpha=7$ deg, $x/c=0.5$, $k=2$

Turbulence velocity profile for different angles of incidence is presented in Figure 19. The increase in angle of incidence

causes increases in turbulence level. Turbulence level starts increasing from the surface of the flat plate (inside the separation region) and reaches its maximum at a height from the surface and then starts decreasing (outside separation region) for each angle of attack.

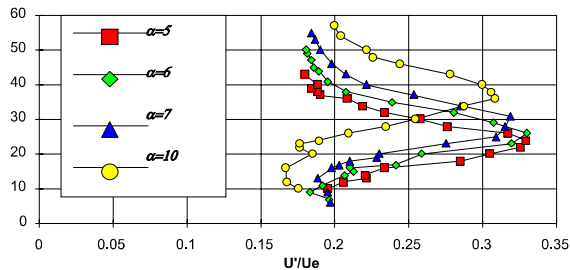


Figure 19 Turbulent fluctuating velocity component for different angles of incidence, $U_e=30\text{m/s}$, $x/c=0.5$, $k=2$

In Figure 20 the variation of Reynolds stress, $\langle U' \cdot U' \rangle$, on top of the wing has been shown for different reduced frequencies. It seems that there is not much changes and the effect of these reduced frequencies in this situation is almost the same.

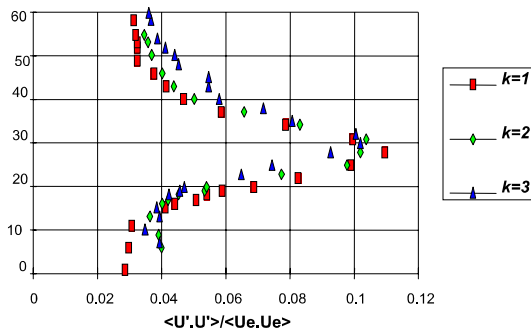


Figure 20 Turbulent variation of Reynolds stress due to different reduced frequencies, $U_e=30\text{m/s}$, $\alpha=7\text{deg}$, $x/c=0.5$

CONCLUSION

A series of experiments have been performed to investigate the characteristics of the turbulent boundary layer separation in steady and unsteady flow over a flat plate in adverse pressure gradient. Pitot-static tube and hot-wire data acquisition were used in measure the ensemble-averaged as well as turbulence velocities over a range of angles of incidence. The main findings are summarized below.

- (i) Freestream velocity distributions in the wind tunnel test section are affected more when closer to the stationary elliptic cylinder.
- (ii) The more the increase in the angle of incidence of the flat plate in steady and unsteady flow, the more is the increase in the thickness of separated region which extends further towards the flat plate trailing edge.
- (iii) The effect of reduced frequency and different freestream velocity seems to be negligible over the upstream

velocity distribution in the wind tunnel test section in the plane of flat plate measured at a particular position.

- (iv) Reduced frequency causes the separation points to move up away from the surface of the flat plate but this movement is restricted to reduced frequencies less than 2 after which the changes are negligible.

REFERENCES

- [1] Williams, J.C.III., and R.Rojas oviedo., Flow development on a joukowski airfoil started impulsively from rest, *Forum on Unsteady Flow Separation ASME CONF*, JUN 1987, pp. 209-214
- [2] Maskell, e.c., Flow separation in three dimension, *Royal Aircraft Establishment, England*, 1995, RAE Report Aero.2565.
- [3] Harvey J.K, and Perry, F.J., Flow field produced by trailing vortices in the vicinity of the ground, *AIAA*, 1971, pp. 1659-1660
- [4] Magarvey, R.H., and Maclathy, C.S., The disintegration of vortex rings, *Can.J.Phys*, 1964, pp. 209-214
- [5] Schneider P.E.M., Sekundarwirbelbildung bei ringwirbeln und in freistrlhen, *Z.Flugwiss.4*, 1980, pp. 307-318.
- [6] Simpson, Roger L., and Agrawal. Naval K., Back flow Structure of Steady and Unsteady Separating Turbulent Boundary Layers, *AIAA J. V28, N 10*, OCT 1990, pp. 1764-1771
- [7] Didden, N., and Ho, C.M., Unsteady Separation in Boundary Layer Produced by an Impinging Jet, *J.Fluid Mech.160*, 1985, pp. 235-256
- [8] Ho, C.M, Unsteady An Alternative Look at the Unsteady Separation Phenomenon, Recent Advances in Aerodynamic A.Krethappalli and C.A.Smith, *Springer-Verlag1986*, pp. 165-178
- [9] Gad.el.hak M., UnSteady Separation on Lifting Surface, *Appl.Mech.*, 1987, pp. 441-453
- [10] Marshal, D. P., and Tansley, C., "An Implicit Formula for Boundary Current Separation", American Meteorological Society, June 2001, Notes and Correspondence, pp.1633-1638
- [11] Vikas Kumar, and Farrukh S.Alvi., Efficient Control of Separation Using Microjet, *35th AIAA Fluid dynamic conference.*, 6-9JUNE 2005, 4879